ELSEVIER

Biochimica et Biophysica Acta 1506 (2001) 67–78

BIOCHIMICA ET BIOPHYSICA ACTA
BBA

www.bba-direct.com

Two-dimensional structure of the native light-harvesting complex LH2 from *Rubrivivax gelatinosus* and of a truncated form

Jean-Luc Ranck [a,*], Teresa Ruiz [a,1], Gérard Péhau-Arnaudet [a], Bernadette Arnoux [b], Françoise Reiss-Husson [c]

[a] *Institut Curie, CNRS-UMR 168, 11 Rue P. et M. Curie, 75231 Paris Cedex 05, France*
[b] *Laboratoire d'Enzymologie et de Biologie Structurale, CNRS, 91198 Gif-sur-Yvette, France*
[c] *Centre de Génétique Moléculaire, CNRS, 91198 Gif-sur-Yvette, France*

Received 13 February 2001; received in revised form 24 April 2001; accepted 24 April 2001

Abstract

The light-harvesting complex LH2 of *Rubrivivax gelatinosus* has an oligomeric structure built from α-β heterodimers containing three bacteriochlorophylls and one carotenoid each. The α subunit (71 residues) presents a C-terminal hydrophobic extension (residues 51–71) which is prone to attack by an endogenous protease. This extension can also be cleaved by a mild thermolysin treatment, as demonstrated by electrophoresis and by matrix-assisted laser desorption-time of flight mass spectrometry. This cleavage does not affect the pigment binding sites as shown by absorption spectroscopy. Electron microscopy was used to investigate the structures of the native and thermolysin cleaved forms of the complexes. Two-dimensional crystals of the reconstituted complexes were examined after negative staining and cryomicroscopy. Projection maps at 10 Å resolution were calculated, demonstrating the nonameric ring-like organization of α-β subunits. The cleaved form presents the same structural features. We conclude that the LH2 complex is structurally homologous to the *Rhodopseudomonas acidophila* LH2. The hydrophobic C-terminal extension does not fold back in the membrane, but lays out on the periplasmic surface of the complex.

Keywords: Antenna; Purple bacterium; Two-dimensional crystal; Oligomeric structure

1. Introduction

In most photosynthetic purple bacteria, absorption of light and its conversion in chemical energy takes place in highly organized, membrane-bound pigment–protein complexes: the light-harvesting I and II antenna (LH1 and LH2) and the reaction center (RC). Several LH1 complexes are tightly associated with one RC, whereas the LH2 are more peripheral and are present in variable amount depending on the growth conditions. Light absorbed by the LH2 pigments is transferred to the LH1-RC core complex. This excitation energy is converted by the RC, where a photoinduced charge separation takes place initiating the cyclic electron transfer chain and the forma-

Abbreviations: LH, light harvesting complex; RC, reaction center; BChl, bacteriochlorophyll; LDAO, lauryl-dimethyl amine oxide; OTG, octyl-thioglucoside; DOM, β-dodecyl maltoside; DOTM, β-dodecyl thiomaltoside; PC, phosphatidylcholine; PE, phosphatidylethanolamine; MALDI-TOF, matrix-assisted laser desorption-time of flight

* Corresponding author. Fax: +33-1-40-51-06-36; E-mail: jean-luc.ranck@curie.fr

[1] Present address: Max-Planck-Institut für Biophysik, Heinrich-Hoffman-Str. 7, Frankfurt/M, Germany.

0005-2728/01/$ – see front matter
PII: S0005-2728(01)00185-2

tion of a chemical potential gradient across the membrane.

In several bacteria, these various complexes have been isolated in a form which conserves their native spectral properties and their activity. The few cases where they could be crystallized improved greatly our understanding of the photosynthetic processes. The structures of the LH2 complexes have been solved to atomic resolution for two purple bacteria, *Rhodopseudomonas* (*Rps.*) *acidophila* [1] and *Rhodospirillum* (*R.*) *molischianum* [2]. These LH2 complexes form cylindrical ring-like assemblies, with a 9-fold or 8-fold symmetry respectively. The repeating motive is a heterodimer of two polypeptides α and β, each containing a single transmembrane α helix, which is roughly parallel to the cylinder axis. The α subunits form the inner part of the ring, and the β ones the outer part. Several pigment molecules are buried in hydrophobic binding sites provided by both subunits. The bacteriochlorophyll (BChl) molecules form two pools with different structures and spectroscopic properties. The BChls which absorb near 850 nm (B850 BChls) form a belt of molecules with their cycles perpendicular to the membrane plane; they are sandwiched between the α and β hydrophobic helices and coordinated by their central magnesium ion to conserved histidines of both subunits. These BChls are tightly coupled and can be described as interacting B850 dimers. The other BChls which absorb at 800 nm (B800) are aligned parallel to the membrane plane, and located between the β hydrophobic helices. They are bound by a residue of the N-terminal part of the α subunit. The carotenoid molecule of each heterodimer is extended in an all-*trans* configuration from the cytoplasmic to the periplasmic surfaces of the complex. In these cyclic structures which are specific for the bacterial antenna, the BChl molecules are positioned very precisely in circular arrays; the effectiveness of such structures for optimizing energy transfer has been pointed out [3]. Two-dimensional (2-D) crystals of *Rhodovolum* (*Rhv.*) *sulfidophilum* [4] and *Rhodobacter* (*Rb.*) *sphaeroides* [5] LH2 also showed, albeit at lower resolution, ring-like assemblies with nonameric symmetry. The structure of a LH1 complex is still unknown to atomic resolution but electron diffraction data of two-dimensional crystals indicate the presence of ring-like structures of a higher, 16-fold symmetry [6]. These larger LH1 rings could accommodate in their internal space one reaction center. Such a model was confirmed by the analysis of two-dimensional crystals of LH1-RC core complexes [7–9]. It is also in good agreement with previous observations done at a lower resolution on *Rhodopseudomonas viridis* intact membranes [10]. In some cases, however, a perfect cyclic arrangement of the LH1 antenna in the core complex has been questioned [11,12]. In vivo, a cyclic organization of the LH2 has still to be demonstrated.

The two polypeptides of *Rubrivivax* (*Rvi.*) *gelatinosus* LH2 possess three domains as all other antenna from purple bacteria: a hydrophobic transmembrane stretch, and more hydrophilic C- and N-terminal parts. As compared to *Rps. acidophila*, the α chain has a C-terminal hydrophobic extension of about 20 residues (Fig. 1), comprising a number of alanine residues in a row. Brunisholz et al. [13] proposed that the extension was folded into a second transmembrane helix, the α subunit spanning the membrane twice (in a 'hairpin' structure). The NH_2 terminus of the β polypeptide is also appreciably longer than in *Rps. acidophila*, while the rest of the sequences is highly homologous. Another distinctive feature concerns the heterogeneity of *Rvi. gelatinosus* LH2 in its carotenoid composition, that reflects the presence of carotenoids of both the spheroidene and the spirilloxanthin series in this bacterium [14]. However, the B850 and B800 BChl molecules, as characterized by resonance Raman spectroscopy, share the same pattern of interactions with their protein binding sites as in *Rps. acidophila* [15].

This LH2 complex has been isolated in a detergent-solubilized form which has kept the native internal energy transfer properties [14,16]. In a previous study, analytical centrifugation was used for determining the oligomeric state of this complex isolated in detergent solution and negatively stained samples were examined by electron microscopy [17]. The centrifugation results were in favor of the existence of heptamers, but the accuracy of this determination strongly depended on the value of the buoyant factor which is difficult to measure. Furthermore the particles observed in the electron micrographs were rod-like, possibly built from stacks of smaller units of a size below the resolution of the images. It was therefore of interest to determine the oligomeric state of this LH2 by a more direct approach, and to

```
α gel          MNQGKVWRVVKPTVGVPVYLGAVAVTALILHGGLLAKTDWFGAYWNGGKKAAAAAAAAAP 60
α acido        MNQGKIWTVVNPAIGIPALLGSVTVIAILVHLAILSHTTWFPAYWQGGVKKAA--------53
               *****:* **:*::*:*. **:*:* *:::* .:*::* ** ***:** * **
α gel           APVAAPQAPAQ 71
α acido         -----------

β gel             MADDANKVWPSGLTTAEAEELQKGLVDGTRIFGVIAVLAHILAYAYTPWLH 51
β acido           ----------ATLTAEQSEELHKYVIDGTRVFLGLALVAHFLAFSATPWLH 41
                           : **: ::***:* ::****:*  :*::**:**:: *****
```

Fig. 1. Sequence comparison of the LH2 polypeptides of *Rvi. gelatinosus* strain S1 (GenBank accession No. AF312921) and *Rps. acidophila* strain 10050. Identical residues are indicated by * and similar ones by :.

examine if the structure differed from the published ones by the presence of a supplementary transmembrane helix. The work reported here describes the structure at low resolution of 2-D crystals as determined by electron microscopy. Native LH2 and a proteolyzed form, where the C-terminal extension of the α subunit has been cleaved, have been examined.

2. Material and methods

2.1. Materials

The following detergents were used: dodecyl-dimethyl amine *N*-oxide (C_{12}DAO, Fluka Biochemica), lauryl-dimethyl amine oxide (LDAO, Fluka 30% solution), octyl thioglucoside (OTG, Sigma), β-dodecyl maltoside (DOM, Sigma) and β-dodecyl thiomaltoside (DOTM, Anatrace). Egg phosphatidylcholine (PC) and egg phosphatidylethanolamine (PE) were purchased from Avanti Polar Lipids.

2.2. Isolation of the LH2 complex

The LH2 complex was isolated from photosynthetically grown *Rvi. gelatinosus* cells (wild type, strain S1) as described previously [14], with several modifications. Namely PMSF was added at 1 mM during the breakage of the cells and the isolation of membranes, which were then washed in a 10 mM Tris–HCl buffer, pH 8.0, containing 1 mM EDTA, 1 mM benzamidine and 5 mM Na ε-aminocaproate. Solubilization of LH2 was done by incubation of the membranes with LDAO for 30 min at 5°C ($A_{857nm} = 50$, 10 mg/ml LDAO) in a 10 mM Tris–HCl, pH 8.0, buffer containing 1 mM EDTA, 1 mM benzamidine–HCl and 5 mM Na ε-aminocaproate (thereafter designated as TEI buffer). The suspension was centrifuged for 2 h at $140\,000 \times g$; the supernatant was adsorbed and washed on a DEAE-Sepharose Fast Flow (Pharmacia) column equilibrated with the TEI buffer containing 1 mg/ml LDAO (designated as TELI buffer). The LH2 complex was eluted with a NaCl gradient (0–0.4 M) in the TELI buffer. The best LH2 fractions (as judged from their IR spectra and minimal A_{280}/A_{854} ratio) were eluted at about 90 mM NaCl. They were pooled, concentrated by ultrafiltration (XM100 Amicon membranes) and repurified by gel filtration on a Sepharose 6B (Pharmacia) column equilibrated and eluted with the TELI buffer. The LH2 fractions were pooled and concentrated by ultrafiltration.

Further purification was achieved by chromatography on a hydroxyapatite column (BioSepra, France) equilibrated with the TELI buffer. The LH2 complex was weakly retained by hydroxyapatite; most of it was eluted by washing with the TELI buffer supplemented with 50 mM phosphate. This chromatography allowed to eliminate weak contaminants of molecular masses higher than 15 kDa, which were eluted (together with the rest of LH2) by raising the phosphate molarity to 0.2 M.

2.3. Limited proteolysis of the LH2 complex by thermolysin

The concentration of LH2 samples obtained after hydroxyapatite chromatography was adjusted to 5 mg/ml and the buffer was exchanged on a Sephadex PD10 (Pharmacia) column for a 10 mM Bis-Tris propane, pH 9.0, buffer containing 1 mg/ml LDAO.

Thermolysin (Boehringer) was added (final concentration 0.1 mg/ml) and the mixture was incubated at 22°C for 4 h. In preliminary experiments the progress of proteolysis was checked by SDS–PAGE electrophoresis. Proteolysis was usually stopped after 4 h by addition of 5 mM EDTA. Thermolysin was eliminated by several cycles of concentration and dilution on a Centricon 100 device, that could be used at the same time for concentrating the protein and/or exchanging the buffer. This LH2 preparation was designated as the truncated LH2.

A few experiments were performed with the same conditions but with chymotrypsin (Sigma) instead of thermolysin.

2.4. Characterization of LH2 after thermolysin proteolysis

The truncated LH2 was analyzed by SDS–PAGE electrophoresis on 16.5% acrylamide gels. It was also characterized by its matrix-assisted laser desorption-time of flight (MALDI-TOF) mass spectrum (see below).

For determining more precisely the polypeptide composition after proteolysis, the α and β subunits were separated by reverse phase HPLC on a Kromasil C4 column (KR5C4-25F, 5 μm gel, 4.6×250 mm). The samples were injected as aliquots (100 μl) of protein in LDAO (1 mg/ml) solution. A linear gradient program was used for eluting the subunits with a flow rate of 1 ml/min, starting from a mixture of acetonitrile/(water/0.1% trifluoroacetic acid (TFA)) 3:7 (v/v) and going to 6:4 (v/v) of the solvent mixture. The column resolved the preparations in two well separated peaks, as detected at 280 nm. The experiment was repeated five times; the corresponding peaks were pooled, dried by vacuum centrifugation and redissolved in a mixture of acetonitrile/(water/TFA 2%) (3:7, v/v). Aliquots were used for mass spectrometry (see below).

2.5. Spectroscopic techniques

Absorption spectra were measured with a Cary 2300 (Varian) spectrophotometer coupled to a personal computer.

MALDI-TOF mass spectrometry was performed with a Bruker Biflex spectrometer. Two types of preparations were used to prepare the matrix-embedded proteins. (1) For LH2 preparations in detergent solutions, the solutions were simply diluted with water before mixing 0.5 μl aliquots with 0.5 μl matrix (a saturated solution of sinnapinic acid in acetonitrile/(2% TFA in water), 3:7 (v/v)). The protein content of the target was 10–50 pmoles. (2) Samples of the individual subunits isolated by reverse phase chromatography were diluted in acetonitrile/(2% TFA in water), 3:7 (v/v) and aliquots were mixed with the matrix as described. Cytochrome *c* and insulin were used for external calibration.

2.6. Biochemical techniques

Samples were prepared for electrophoresis by acetone/methanol (7:2, v/v) precipitation, dissolution of the precipitate in a sample buffer containing 63 mM dithioerythritol, and heated for 10 min at 60°C. SDS–PAGE was performed on 0.75 mm thick minigels using 16.5% acrylamide [18]. Gels were stained with 0.25% Coomassie blue R-250.

Protein concentration was measured with the bicinchoninic acid reagent (Pierce) after acetone/methanol (7:2, v/v) precipitation. It was also estimated from the absorbance at 854 nm, using $\varepsilon = 382\ \mathrm{mM}^{-1}\ \mathrm{cm}^{-1}$ [14] and values of 12 530 Da and 10 933 Da for the molecular masses of the native LH2 and of the truncated one (see Section 3).

2.7. Preparation of 2-D crystals

LH2 in 10 mM Tris, 300 mM NaCl, 25 mM $MgCl_2$ and 0.1% LDAO at pH 8.0 was mixed with various amounts of lipid containing solutions (5 mg/ml solution) to give a final weight ratio of lipid per protein ranging from 0.3 to 0.5. Lipid containing solutions 1 and 2 consisted respectively of egg PC and egg PC/egg PE (50:50, w/w) in water. The final protein concentration ranged from 0.2 to 0.7 mg/ml. After 2 h incubation at room temperature in the dark, the detergent was removed by repeated treatment with polystyrene beads (Biobeads SM2 from Bio-Rad, USA) for 4 h. The 2-D crystallization was monitored, as a function of time, by electron microscopy. The samples were stable in the dark at 4°C for several weeks.

2.8. Electron microscopy and image analysis

Aliquots of approx. 5 μl of LH2 2-D crystals were deposited on carbon coated grids, blotted and negatively stained with several drops of a 1% solution of uranyl acetate, air dried and immediately used for electron microscopy. Micrographs (SO-163 Kodak, France) were collected with a Philips CM120 electron microscope equipped with a LaB6 filament operating at 120 kV. Low dose images were recorded at nominal magnification of 45 000 and an electron dose of approx. 5 $e^{-}/Å^2$. Negatives were developed for 12 min in full-strength developer Kodak D-19. For cryomicroscopy, LH2 2-D crystals were deposited on carbon coated grids, blotted and frozen by plunging into liquid ethane on an EMCPC freezing device (Leica, France). The cryospecimens were transferred immediately to a Gatan 626 cryoholder and examined on a Philips CM120 under the same conditions as the negatively stained samples. Micrographs were evaluated for defocus, astigmatism and drift by optical diffraction prior to analysis. The selected areas of interest were digitized on a Leafscan 45S CCD array microdensitometer (Leaf System). The sampling was 0.4 nm on the specimen scale. Areas were padded up to 1024 or 2048 pixels square. Lattice parameters were determined using the program Spectra [19]. The data were further processed using the MRC image analysis package [20]. Data from several crystals were merged and projection maps were calculated subsequently.

3. Results

3.1. The C-terminal extension of the α subunit is readily cleaved by an endogenous exoprotease, without influence on the absorption spectrum of LH2

Fig. 2 shows the room temperature absorption spectrum of the LH2 complex obtained after gel filtration. The Soret band of the BChls, their Q_x and their two Q_y transitions are located at 370, 585, 802 and 854 nm respectively; the absorption maxima at 460, 487 and 518 nm are attributed to the various carotenoids known to be present in this complex [14]. The low UV absorption (as compared to the near infrared one) is indicative of the purity of the preparation. The SDS–PAGE analysis (not shown) revealed the two LH2 polypeptides, migrating with apparent molecular masses of 8 and 6 kDa and minor contaminants of higher molecular mass. These contaminants were eliminated after the hydroxyapatite chromatography (Fig. 3).

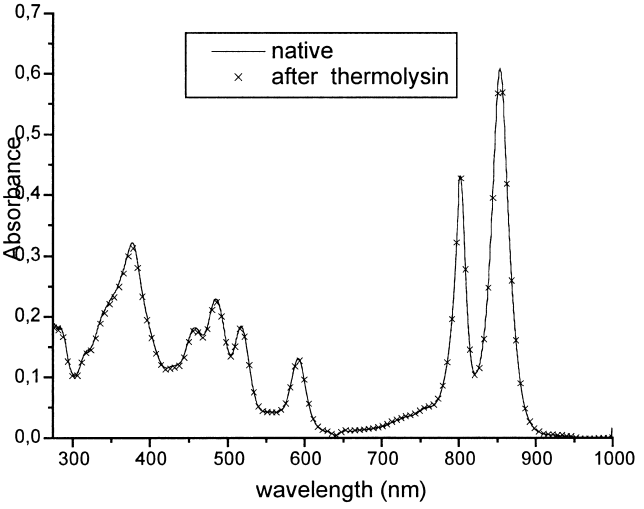

Fig. 2. Absorption of LH2 preparations in a 10 mM Bis-Tris propane buffer, pH 9.0, containing 1 mg/ml LDAO, before thermolysin proteolysis (———) and after 4 h thermolysin treatment (×).

We noticed that the SDS–PAGE pattern was modified within a few days of storage at 5°C if protease inhibitors (and particularly EDTA) were not present during the purification. Under these conditions, another band was observed between those corresponding to the α and β polypeptides; its staining increased at the expense of the α band and eventually replaced it as the sample aged. The β band was not affected and the absorption spectrum was not altered (not shown). The addition of protease inhibitors during the purification (as described in Section 2) prevented this modification of the α subunit.

In the MALDI-TOF mass spectra of LH2 isolated in the presence of protease inhibitors and after hydroxyapatite chromatography, two sharp peaks were observed at $m/z = 7118$ and 5427, without other intermediate species (Fig. 4). The first could be identified with the intact α subunit (αMet1-Gln71, $M = 7107$); the second one corresponded to the β subunit processed by removal of its N-terminal Met (βAla2-His51, $M = 5423$). In the absence of in-

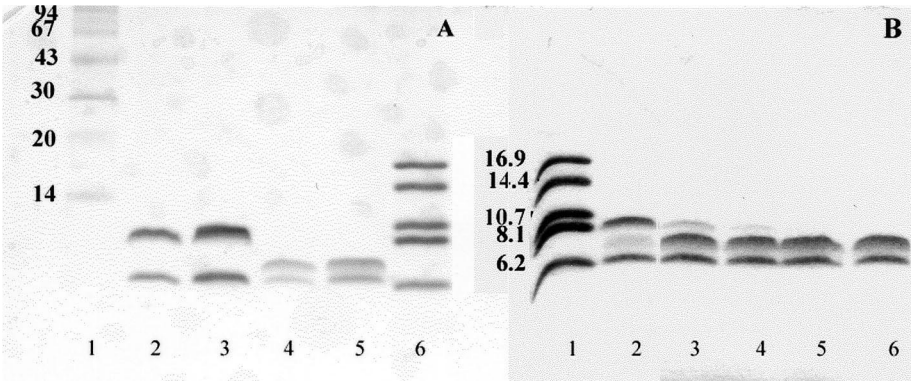

Fig. 3. SDS–polyacrylamide minigels (16.5% polyamide) of LH2 preparations. (A) Lanes: 1 and 6, molecular mass markers; 2 and 3, native LH2; 4 and 5, LH2 after thermolysin proteolysis. (B) Time course of the proteolysis by thermolysin; the incubation was performed as described in Section 2. Lane 1 (left), molecular mass markers. Lanes 2–6, aliquots taken respectively at incubation times zero, 30 min, 1 h, 2 h and 4 h.

hibitors, supplementary peaks were observed (not shown). The major one corresponded to $m/z = 6446$, and minor ones were observed in a series from $m/z = 5941$ to 5585, differing from each other by $m/z = 71$ (which corresponds to the removal of one Ala residue). According to the primary sequence of the α subunit, the major band could be identified with αMet1-Ala64 ($M = 6443$), and the minor ones to successive cleavages of the terminal Ala residues, leading from αMet1-Ala58 ($M = 5943$) to αMet1-Ala53 ($M = 5582$). These results demonstrated that the hydrophobic C-terminal extension of α was gradually split off by an exoprotease which removed first the last seven residues of the C-terminus, then went on by single steps until the 18th last one.

During the amino acid sequencing of the LH2 antenna from another *Rvi. gelatinosus* strain, Brunisholz et al. observed also that in one of their LH2 preparations the 16 last C-terminal residues of α were lacking [13], an observation consistent with ours. They also noticed that the absorption spectrum did not change.

3.2. Limited proteolysis of LH2 by thermolysin cleaves the C-terminal extension of the α subunit

The spontaneous proteolysis of α observed in the absence of inhibitors led to a very heterogeneous population of LH2 complexes, a situation detrimental for structural studies. We tried therefore to deliberately cleave the C-terminal extension by a foreign protease, while leaving intact the other subunit. Such a modification was also of interest for determining if this extension had any role in the oligomeric structure of the LH2.

A few unsuccessful experiments were done with chymotrypsin as described in Section 2; after incubation at 20°C during 2 h we did not observe any modification of the SDS–PAGE electrophoresis profile. We turned then to a short incubation with thermolysin. With this protease a new band migrating between the α and β ones was detected on SDS gels; it replaced the α band after 2 h incubation, while the migration of the β subunit was not affected (Fig. 3B). This treatment did not modify the absorption spectrum (Fig. 2).

The MALDI-TOF mass spectra of samples after 4 h treatment with thermolysin confirmed that the α subunit was modified: only one broad and poorly resolved band peaking at $m/z = 5430$ with several shoulders was observed (Fig. 4) which could correspond to the modified α subunit superimposed on the β one.

In order to clarify the site(s) of cleavage, the separation of the subunits of the truncated LH2 was done by reverse phase HPLC after pigment removal, following a method already published [13]. This chromatography resolved the preparation in two fractions which were separately examined by mass spectrometry. The fraction which was eluted the last by the solvent gradient contained as major peak a species of $m/z = 5420$ (not shown): it was thus identified as the β (Ala2-His51) subunit. For the other fraction a broad and noisy spectrum was

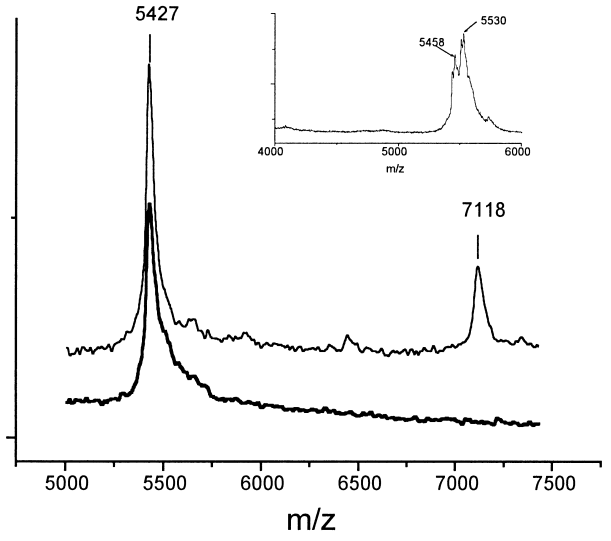

Fig. 4. MALDI-TOF mass spectrometric analysis of various LH2 preparations. Y axis: intensity in arbitrary units. Spectra obtained with native LH2 (———) and thermolysin treated LH2 (———) in LDAO solution have been superposed. (Insert) MALDI-MS spectrum of the α subunit isolated by HPLC after thermolysin proteolysis.

observed, with several maxima in the range of m/z = 5430–5530 (Fig. 4). A comparison with the polypeptide sequence revealed that it could be a mixture of derivatives of the α polypeptide originating from cuts after Ala51 and Ala52 (M = 5440 and 5511 respectively). Therefore in the truncated LH2 most of the hydrophobic C-terminal extension of α subunit was removed, leaving intact the rest of this polypeptide and the whole β subunit. The homogeneity of this preparation was higher than after spontaneous proteolysis.

3.3. *Formation and structural analysis of the LH2 2-D crystals*

The 2-D crystals of LH2 were found over a large range of conditions. Their appearance was highly dependent on the nature of the detergent (see Fig. 5). The first preparations of native LH2 complexes purified in the presence of DOM and screened for crystal formation were not successful. Thereafter C_{12}DAO was used instead of DOM, but the formation of 2-D crystals was still hazardous and of poor quality. The best results were obtained with LDAO, probably due to the larger dispersity of the hydrocarbon chain length (indeed it is known that the commercial detergent sold as LDAO contains a mixture of C_{12} and C_{14} alkyl chains). Exchanging the detergent by diluting LDAO with other detergents like OTG or DOTM resulted in much larger vesicles. However, the diffraction of these samples was not significantly improved compared to the standard protocol.

After screening a wide variety of lipids (synthetic, natural, neutral or charged) we observed that the best crystals were obtained either with egg PC or a mixture of egg PC and PE (50:50, w/w). These crystals were at lipid to protein ratios in the range of 0.3–0.5 (w/w), although ordered arrays of variable quality could be obtained with lipid to protein ratios in the range of 0.2–1.2. No color change occurred during the time of experiments, even after weeks at 4°C in the dark, indicating a strong attachment between the pigments and the α and β subunits. This has been confirmed by recent measurements of the absorption spectra of the preparations (S. Scheuring et al., to be published).

The concentration of sodium chloride was critical and below 300 mM the crystals did not form. Magnesium chloride added to the crystallization medium did not improve the quality, but favored the formation of larger arrays. Therefore the concentration of magnesium chloride was kept at 5 mM in further reconstitution trials. The rate of detergent removal can often be modulated by temperature or by the amount of biobeads added. However, slow or fast detergent removal conditions (low temperature/small amount of biobeads or high temperature/large amount of biobeads, respectively) did not play a significant role. Room temperature and 4 h stirring in the presence of polystyrene beads were standard conditions. The crystallization assays on the truncated LH2 complexes did not require special conditions to form 2-D crystals (Fig. 5C). The same crystallization conditions applied to this kind of LH2 preparation were successful. Vesicles and sheets, made of several layers, were observed but only a small number of these structures showed ordered domains. This forced us to collect a large number of micrograms to obtain a sufficient number of good images. In vitreous ice, only a small number of well order crystals could be preserved. This prevented us from collecting sufficient data from frozen hydrated samples for the current analysis. Our studies are focused on the dif-

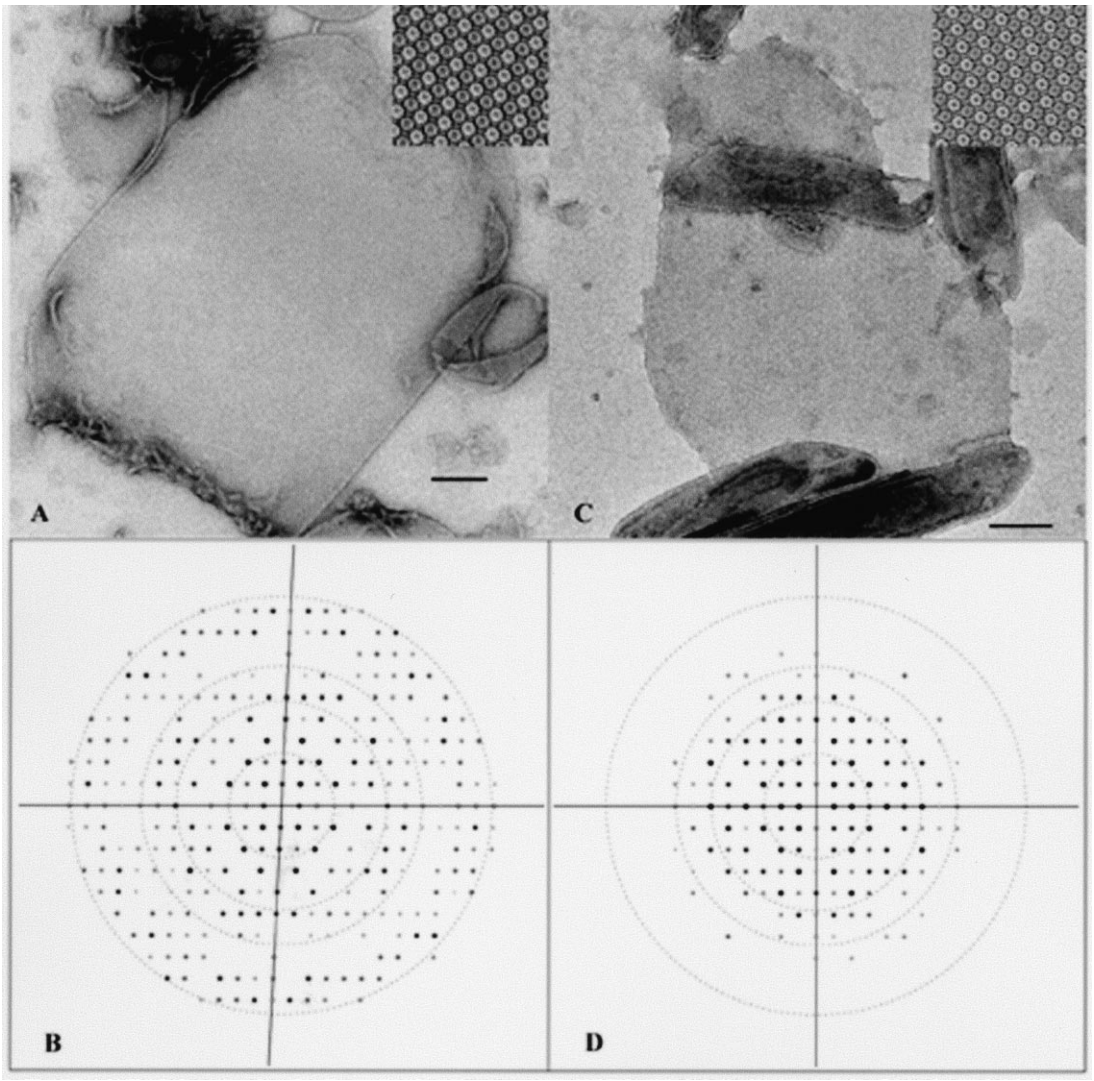

Fig. 5. (A) Low dose electron microscopy of two-dimensional crystals of native LH2 complexes from *Rvi. gelatinosus*. Insert shows filtered image from masked Fourier transform (B) of electron microgram. Bar = 100 nm. (C) Low dose electron microscopy of two-dimensional crystals of truncated LH2 complexes from *Rvi. gelatinosus*. Insert shows filtered image from masked Fourier transform (D) of electron microgram. Bar = 100 nm.

ferences between the truncated and wild LH2; these differences could be clearly resolved in our negatively stained preparations.

The collapsed vesicles, from optical diffraction observations, often showed two sets of sharp and strong diffraction spots. Micrograms where the two lattices could be indexed without overlapping from each other have been used subsequently. Frequently, in the same sample, we observed two major crystals forms. Form 1 is monoclinic with unit cell parameters $a = 90$ Å, $b = 120$ Å and $\gamma = 92°$. Form 2 is hexagonal with an unique cell parameter $a = b = 66$ Å and $\gamma = 60°$. Sometimes a larger form, 3, appeared, which is monoclinic with cell parameters $a = 75$ Å, $b = 175$ Å and $\gamma = 92°$. This polymorphism is not related to special crystallization conditions and was observed in the crystallization of native LH2 complex as well as truncated ones; the lattice dimensions of the various forms did not depend on the LH2 sample, whether truncated or not.

The monoclinic lattice, form 1, shows an upside-down repetition (Fig. 5, insert). The Fourier transform of the raw data from native crystal shows diffraction spots to a resolution of 10 Å, indicating an

almost perfect alignment of the crystal domains (see Fig. 5B). The hexagonal lattice, form 2, corresponds to an arrangement of LH2 rings oriented in the same direction. The resolution limits of form 2 and form 3 are 15 and 20 Å respectively. For image analysis, only the best images from monoclinic lattices (form 1) were selected and processed. No unbending was applied to the native LH2 crystals and only the best Fourier transforms were selected to proceed with the image analysis. From 12 images selected after origin determination, eight were merged and averaged. Fig. 6A and C show projection maps and IQ plots from raw data of the native and truncated LH2 complexes. LH2 complexes arrange in a ring built from nine α-β subunits corresponding one by one to the density peaks on the projection maps. The same structure

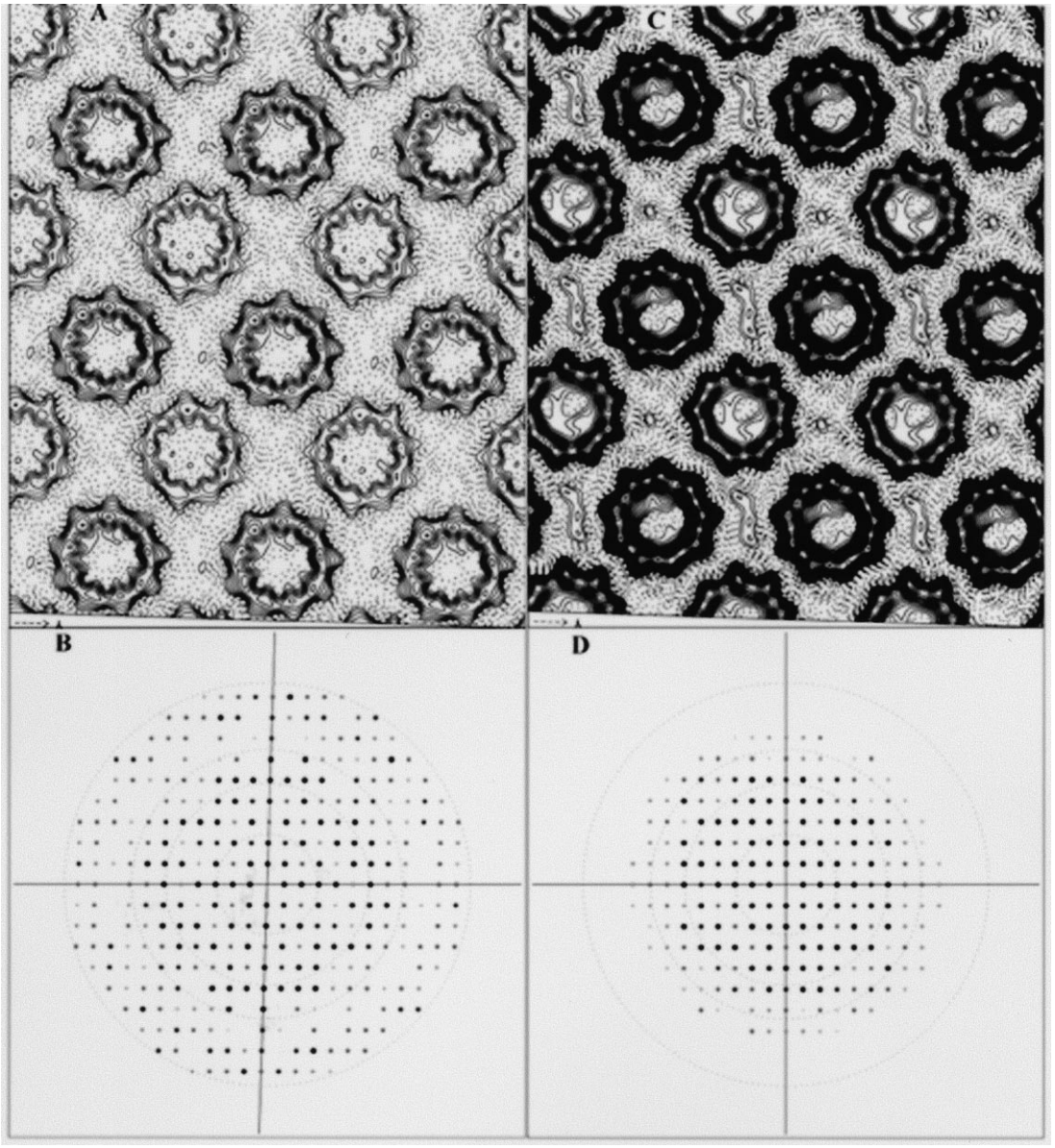

Fig. 6. Projection maps (A,C) after processing and averaging of negatively stained native and truncated two-dimensional crystals of LH2 complexes from *Rvi. gelatinosus*. Diffraction properties of the corresponding native (B) and truncated (D) LH2 complexes from *Rvi. gelatinosus*. Plot B shows the Fourier transform of eight negatively stained images after processing and merging. Plot D shows the Fourier transform of four negatively stained images after processing and merging. The size of the circles indicates the IQ values. The dotted rings are at radii corresponding to 1/40, 1/20, 1/15 and 1/10 $Å^{-1}$ from the center.

is revealed for the truncated LH2 complex by the projection map despite the lower resolution (about 15 Å) of each image analyzed.

4. Discussion and conclusion

From the biochemical characterization of the isolated LH2 complex reported in this work we can conclude that a limited proteolysis by thermolysin allows to cleave selectively the C-terminal extension of the α subunit without any consequence on the spectral properties of the complex. The removal of the α residues from Ala51-Ala52 to Gln71 did not seem to modify the BChls and carotenoid binding sites, implicating that these residues are not engaged in any interactions with the pigments. In the detergent-solubilized state, the hydrophobic part of the protein is shielded by a detergent belt, and presumably more protected than the hydrophilic surfaces from a proteolytic attack by a soluble enzyme. The preferential cleavage of the C-terminal extension, at least under the conditions we described, suggests that it is readily accessible at the surface of the protein–detergent complex (that is, exposed in vivo on the periplasmic surface). In the homologous *Rps. acidophila* LH2, the residues αAla51 and αAla52 are at the C-terminus (cf. Fig. 1) and they are considered mobile; indeed the α chain is not defined in the electron density map from Gly47 to Ala52 [21]. Long term exposures of detergent-solubilized LH2 antenna from other bacterial species (*Rps. acidophila* and *Rhodocyclus tenuis*), to various proteases (not including thermolysin), have been reported [22,23]; these extensive digestions resulted in progressive spectral shifts and in the cleavages of the C-terminal domains of both subunits. Here we adopted a more gentle procedure, as to restrict the cleavage to the hydrophobic extension of the α subunit and to let intact the structure of the antenna, as shown by the analysis of the 2-D crystals.

The reconstitution of the complex in lipid bilayers and the formation of 2-D crystals did not modify the molecular assembly of the LH2 complex; spectroscopic properties did not show any shift or loss of absorption peaks, indicating the integrity of all the pigment binding sites. More importantly, the truncated LH2 complex behaved before and after reconstitution exactly as the native one with the chromophores still firmly attached to the α and β subunits. Both native and truncated LH2 showed clearly the same nonameric structure from projection maps of negatively stained 2-D crystals (Fig. 6) and of unstained frozen ones (not shown). The ring size evaluated from these maps is closely related to those deduced from the X-ray structures of *Rps. acidophila* [1] and *R. molischianum* LH2 [2]; both inner and outer diameters of the ring measured on the electron microscopy projection maps are in good agreement with those calculated from the X-ray diffraction studies (Table 1). Projection maps from negatively stained 2-D crystals (at the difference from unstained frozen ones) only originate from the part of the structure which is accessible to the stain. Thus they represent mainly the exposed surfaces of the LH2 complex. We tried therefore to identify this surface, i.e. as periplasmic or cytoplasmic. Correlation coefficients were calculated between the projection maps obtained from the crystallographic model of *Rps. acidophila* [1] and the projection map obtained from electron micrograms. To this end, the projection maps of the crystallographic model were systematically turned around the axis perpendicular to the plane of the projection. This type of calculation was carried out applying different masks/parameters. On average the correlation coefficients of the optimized orientations at the pair A/B (Fig. 7) and the pair C/D are 0.66 and 0.65. Thus they are close. However, the

Table 1
Comparison of the diameters of the nonameric ring measured in the projection maps by electron microscopy and the corresponding diameters measured from X-ray data for *Rps. acidophila* LH2

	Negative staining[a]	Cryomicroscopy[a]	X-Ray data[b]
Native			
External	68 Å	70 Å	
Medium	48 Å	50 Å	
Internal	28 Å	30 Å	
Truncated			
External	70 Å	70 Å	72 Å
Medium	49 Å	50 Å	50 Å
Internal	30 Å	30 Å	30 Å

[a]Diameters estimated from projection maps of electron microcopy (the external and internal diameters are slightly dependent on the choice of the threshold).
[b]Diameters calculated from projection on a plane of X-ray data (taken from Protein Data Bank ref. 1KZU).

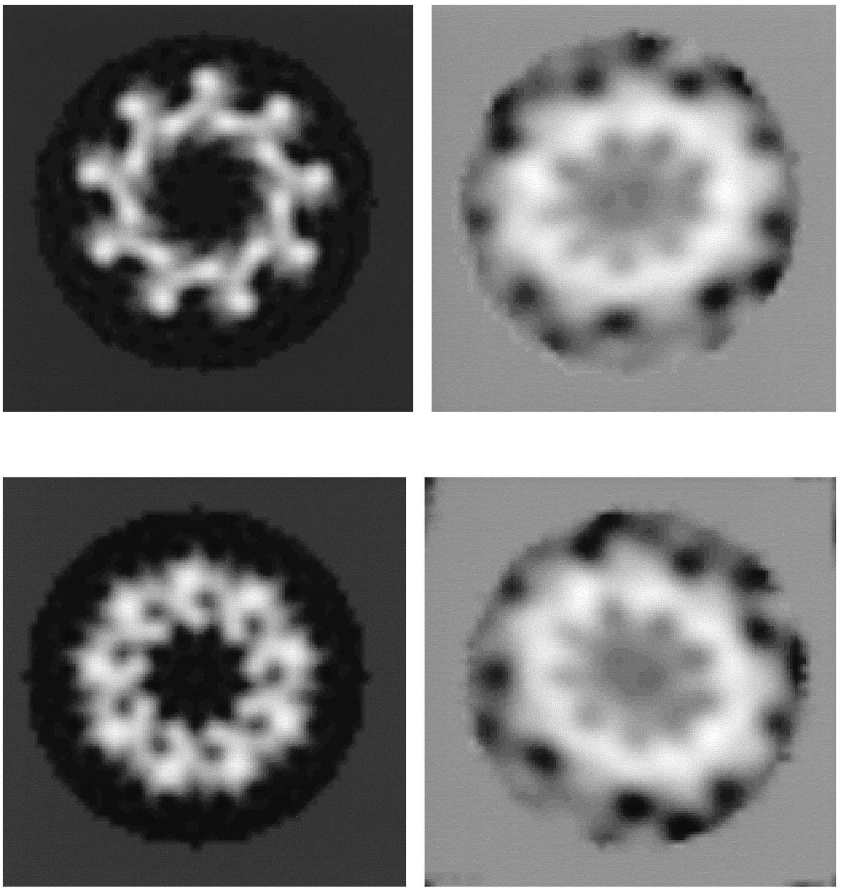

Fig. 7. The top panels (A,C) depict projection maps calculated from the model of the *Rps. acidophila* LH2 structure determined by X-ray crystallography [1]. The top left projection map (A) was calculated based on a model retaining only the part of the structure which is located at the periplasmic surface; the part of the structure within the membrane and on the cytoplasmic surface was deleted from the model. The top right projection map (C) was calculated by retaining in the model only the part of the structure located at the cytoplasmic surface. The bottom panels (B,D) represent projection maps calculated from the electron micrograms.

correlation coefficients of the pair A/B are always better than those of the pair C/D. The outer and inner diameters of the projection are closer for the pair A/B than for the pair C/D. Furthermore, the more pronounced corrugated character of the outer line delimiting the projection in Fig. 7 (top left) fits better to the corresponding line in Fig. 7 (bottom left). For these reasons we conclude that the projection map calculated from the electron micrograms was obtained from the periplasmic part of the LH2 complex.

We may note that in the 2-D crystals from negatively stained samples as well as from unstained, frozen ones (not shown) the rings are not closely packed and do not make contact with neighboring ones. As already discussed by Walz et al. [9], this loose packing might explain the lower ordering observed here as compared to the better resolution obtained for 2-D crystals of *Rb. sphaeroides* LH2.

When results obtained with the native LH2 or with the truncated one were compared, no extra density could be localized on the projection map of the native LH2 complex either inside or outside the ring, nor, according to the point mentioned before (Table 1), did the ring size show a significant increase to allow the positioning of an extra α helix inside or outside the barrel constituted by the nine α-β subunits of the LH2 complex. The absence of important modifications of the truncated LH2 projection map is in favor of the periplasmic localization of the extra 21 amino acids of the α C-terminus. Therefore the 'hairpin' structure proposed for the α subunit by

previous authors [13] is ruled out by our results, which support the structural homology of *Rvi. gelatinosus* LH2 to that of *Rps. acidophila*. This homology extends to other LH2 structures also obtained by electron microscopy for *Rhv. sulfidophilum* [4], and for *Rb. sphaeroides* [9].

Coming back to the heptameric state proposed previously for LH2 in C_{12}DAO solution [17], a possible explanation would invoke uncertainties in the interpretation of the sedimentation analysis, which could increase the error estimated for the oligomeric degree (which was given as 7.0 ± 0.6). It should also be noted that no crystals could be obtained when the LH2 complex was isolated and maintained in C_{12}DAO solution.

Interestingly, the truncated LH2 complex behaves like the native one from the crystallization point of view and the spectroscopic properties are quite similar. These facts seem to confirm the absence of 'implication' of the extra 21 amino acid fragment in the process of light transmission; it does not seem to intervene in the interactions between heterodimers and in oligomerization. The biological role of this extension is not known; it might be noted that the LH1 complex from the same bacterium presents a similar extension at the gene level, which is processed and absent in the mature protein [24].

The structural interpretation that we propose in this work, based on electron microscopy by LH2 2-D crystals, has been confirmed recently by atomic force microscopy experiments, which are described in a forthcoming paper (S. Scheuring et al., to be published).

Acknowledgements

This work was supported by the CNRS program 'Physique et Chimie du Vivant'. We thank Dr. P. Bron for help in calculating correlation coefficients, J.P. Le Caër for his help in preliminary mass spectrometry experiments, and J.L. Rigaud for support.

References

[1] G. MacDermott, S.M. Prince, A.A. Freer, A.M. Hawthornethwaite-Lawless, M.Z. Papiz, R.J. Cogdell, N.W. Isaacs, Nature 374 (1995) 517–521.
[2] J. Koepke, X. Hu, C. Muenke, K. Schulten, H. Michel, Structure 4 (1996) 581–597.
[3] A. Freer, S. Prince, K. Sauer, M. Papiz, A. Hawthornwaite-Lawless, G. McDermott, R. Cogdell, N.W. Isaacs, Structure 4 (1996) 449–462.
[4] H. Savage, M. Cyrclaff, G. Montoya, W. Kûhlbrandt, I. Sinning, Structure 4 (1996) 243–252.
[5] T. Walz, S.J. Jamieson, C.M. Bowers, P.A. Bullough, C.N. Hunter, J. Mol. Biol. 282 (1998) 833–845.
[6] S. Karrasch, D. Typke, T. Walz, M. Miller, G. Tsiotis, A. Engel, J. Mol. Biol. 262 (1996) 336–348.
[7] I. IkedaYamasaki, T. Odahara, K. Mitsuoka, Y. Fujiyoshi, K. Murata, FEBS Lett. 425 (1998) 505–508.
[8] H. Stahlberg, J. Dubochet, H. Vogel, R. Ghosh, J. Mol. Biol. 282 (1998) 819–831.
[9] T. Walz, R. Ghosh, J. Mol. Biol. 265 (1997) 107–111.
[10] K.R. Miller, Nature 300 (1982) 53–55.
[11] C. Jungas, J.L. Ranck, J.L. Rigaud, P. Joliot, A. Vermeglio, EMBO J. 18 (1999) 534–542.
[12] F. Francia, J. Wang, G. Venturoli, B.A. Melandri, W.P. Barz, D. Oesterhelt, Biochemistry 38 (1999) 6834–6845.
[13] R.A. Brunisholz, F. Suter, H. Zuber, Eur. J. Biochem. 222 (1994) 667–675.
[14] V. Jirsakova, F. Reiss-Husson, B. VanDijk, G. Owen, A.J. Hoff, Photochem. Photobiol. 64 (1996) 363–368.
[15] J.N. Sturgis, V. Jirsakova, F. Reiss-Husson, R.J. Cogdell, B. Robert, Biochemistry 34 (1995) 517–523.
[16] V. Jirsakova, Thesis, Université de Paris-Sud, Orsay, 1995.
[17] V. Jirsakova, F. Reiss-Husson, J.L. Ranck, Biochim. Biophys. Acta 1277 (1996) 150–160.
[18] H. Schägger, G. Von Jagow, Anal. Biochem. 166 (1987) 368–379.
[19] M.F. Schmid, R. Dargahi, M.W. Tam, Ultramicroscopy 48 (1993) 251–264.
[20] R.A. Crowther, R. Henderson, J.M. Smith, J. Struct. Biol. 116 (1996) 9–16.
[21] S.M. Prince, M.Z. Papiz, A.A. Freer, G. Mc Dermott, A.M. Hawthornthwaitelawless, R.J. Cogdell, N.W. Isaacs, J. Mol. Biol. 268 (1997) 412–423.
[22] R.A. Brunisholz, H. Zuber, Photochem. Photobiol. 57 (1993) 6–12.
[23] Q. Hu, R.A. Brunisholz, H. Zuber, Photosynth. Res. 50 (1996) 223–232.
[24] K.V.P. Nagashima, K. Matsuura, S. Ohyama, K. Shimada, J. Biol. Chem. 269 (1994) 2477–2484.